Slide in Overconsolidated Clay below Embankment

Glissement dans une Argile Surconsolidée sous Remblai

N.JANBU The Norwegian Institute of Technology,
O.KJEKSTAD Norwegian Road Research Laboratory (Now NGI),
K.SENNESET The Norwegian Institute of Technology, Norway

SYNOPSIS This paper deals with a slide which took place during construction of a road embankment placed on a slope of overconsolidated clay. Extensive field and laboratory investigations of the soil conditions in and around the slide area gave reliable data for a detailed study of this interesting case record. The overall findings lead to the following conclusion:

- The slide is best explained in terms of effective stress analyses based on average effective shear strength parameters determined by undrained triaxial tests, and excess pore pressure estimated from the effective stress paths. The shape and location of the critical shear zones, where $F_{min} \approx 1.0$, is similar to the observed failure surface.
- A total stress analysis, using undrained shear strength (s_u) determined by unconfined compression and fall cone tests, leads to critical shear zones very different from the observed failure surface, and a reliable average value for F_{min} is difficult to obtain because of the very large scatter in measured s_u-values.

The above conclusions are of particular interest because this case record deals with a short-term, undrained load on a fully saturated, fairly intact clay.

INTRODUCTION

On August 15., 1972 a slide of some 160.000 m³ took place beneath a road embankment placed on a slope of overconsolidated clay, about 4 km south of downtown Trondheim.

The sandwich fill embankment was part of a rerouting operation for the main highway E6 out of Trondheim, south to Oslo. See photo in Fig. 1.

Fig.1 Photo of slide

In a joint venture the Norwegian Road Research Laboratory in Oslo, and the Soil Mechanics Institute at NTH in Trondheim undertook to investigate the causes of the slide in order to obtain a basis for the redesign of the embankment. This paper is based on extensive investigations made by these two organizations.

The location of the slide area is shown on the simplified map and plan in Fig. 2a. and b. The existing highway E6 out of Trondheim and the new route are both indicated on the map.

The sandwich embankment on the east side of the Kroppan Ridge was started up on June 5., 1972 and by Aug. 15. some 26.000 m³ were in place. The top soil had been removed in 1971, and the toe rock fill was also placed in the summer of 1971.

On August 15. the embankment was completed up to about elevation 30. A bulldozer driver was working on the embankment a little before 3 pm when he noticed a crack slowly developing on top of the fill. He put a matchbox in the joint. When the matchbox fell into the growing crack, he quickly moved westward on to original ground. Thus he was able to see the slide

taking place from his "orchestra seat".

The soil cracking and the movement of the slide was fully completed in about 10 minutes according to the eye witness.

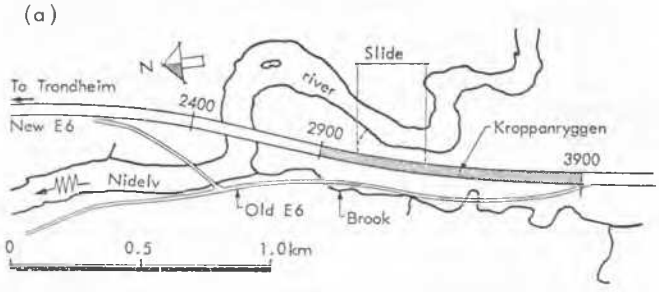

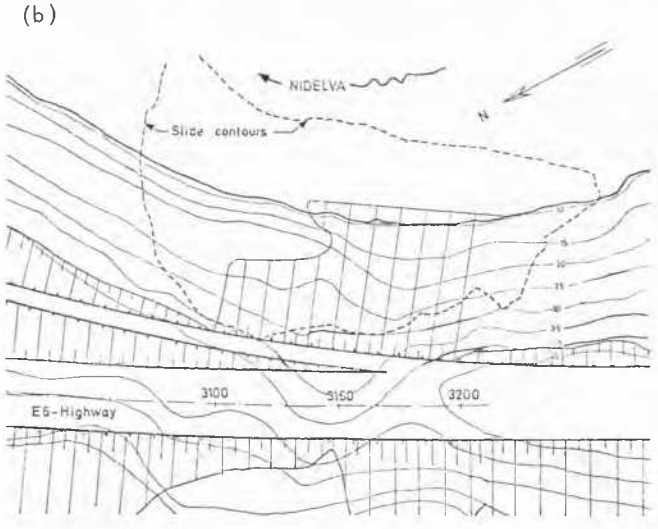

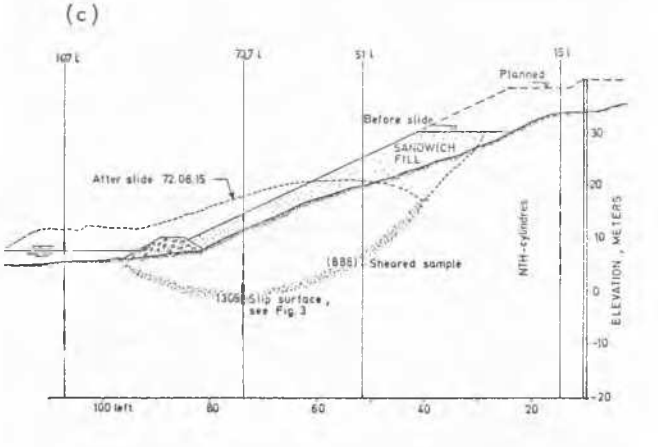

Fig.2 Map , plan , profile

The length of the slide along the highway is roughly 160 m, and the downward slump is more than 10 m in average. Fig. 2c. represents a profile across the slide at mark 3150. The location of the four borings along this profile, and the elevations of the triaxial test samples in each boring are also shown on the profile.

Based on several observations when samples were opened, and based on geometry studies of the profiles before and after the slide, the location of the sliding surface is well established, as indicated in Fig. 2c. It was particularly interesting to find that the slip surface could be so easily observed in sample No. 1305 during extrusion from the tube, see photo in Fig. 3.

Fig.3 Photo of extruded sample No. 1305

SITE INVESTIGATION

The Road Research Laboratory carried out the extensive site investigation after the slide. A routine soil investigation prior to the embankment design had established that the subsoil was stiff, overconsolidated clay, with an estimated design safety of about 1.4 based on s_u-analyses.

In addition to profiling and geodetic survey, the site investigation comprised:

Static soundings, 46 boring
Sampling, NGI 54 mm, 11 borings,
Vane tests, 3 holes,
Pore pressure measurements, 9 holes,
Settlement observations.

The borings were placed mainly along Profiles 3100, 3150 and 3200, with a concentration along 3150. A few borings were placed outside the slide area. The depth of continuous sampling was about 30 m in 6 of the borings, and from 6 to 23 m in the remaining 5 holes.

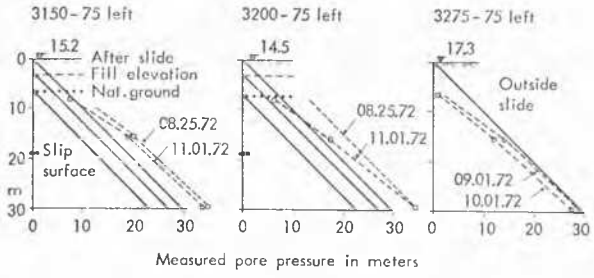

Fig.4 Pore pressure observations

The results of the pore pressure measurements are illustrated in Fig. 4, by dashed lines, as compared to the equivalent hydrostatic pressure (at 1:1) given on the figure from 3 elevations: original ground, fill elevation on Aug. 15., and the terrain after the slide. Inside the slide excess pore pressure of some 5 m above terrain was established, slowly diminishing. On the hillside outside the slide, a decrease in pore pressure of 2 to 3 m, was established over a few days, and remained fairly stable for several months, with only a slight increase in pore pressure over that period.

Settlements up to 10 cm developed along the sliding mass of the toe in the course of 3 months, after which the toe started to heave at an initial rate of about 1 cm/month. This heave slowed down appreciably over the next few months.

LABORATORY INVESTIGATION

The extent of the laboratory soil testing program is illustrated by the following short summary:

some 140 meter of soil contained in about 175 steel cylinders (NGI 54 mm)

were shipped to the laboratories. For each cylinder 2-6 determinations were made for water content and undrained shear strength, and 1 to 2 unit weight measurements and sensitivity determinations. In addition grain size distributions, liquid limit, and plasticity determinations were made on a large number of samples. This very extensive soil testing (4000 results) was carried out primarily at the Road Research Laboratory.

From 14 preselected cylinders 35 samples were obtained for triaxial tests (CU), and 7 of the cylinders were X-rayed for identification of stratification or possible slip zones. This investigation was carried out at the Soil Mechanics Laboratory, NTH.

Overall soil condition

The Kroppan Ridge consists of post glacial marine sediments, predominantly overconsolidated clay. Locally, however, there are a number of erratic features encountered in the subsoil conditions, mainly due to meanderings of the Nidelv river, old sliding activity, and secondary deposits.

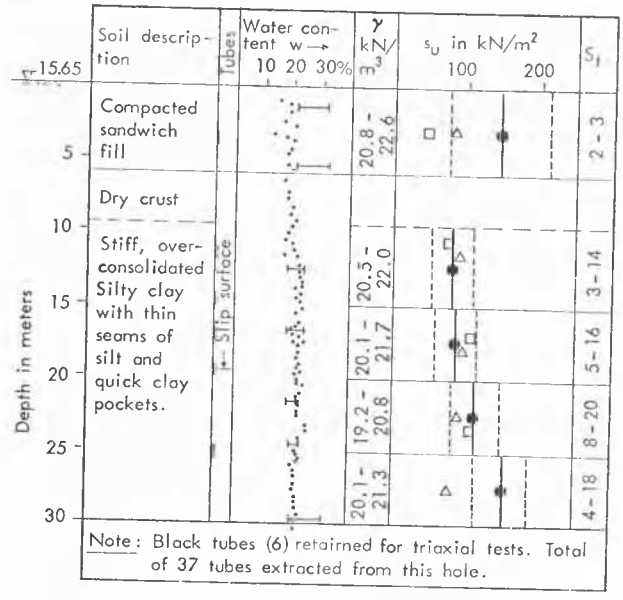

Fig.5 Simplified soil profile at 3150 - 71.4 left

A simplified summary of typical soil data is found in Fig. 5 for the borehole 73.7 m left of the E6 centerline in Profile 3150. As a whole the index properties of the soil are remarkably constant, as illustrated by these approximate values for the overconsolidated clay:

water content	=	22-25%
plastic limit	=	18-21%
plasticity index	=	3- 7%
sensitivity	=	3- 8
unit weight	=	20-21 kN/m³
clay content	=	15-25%

An overall judgement would lead to the conclusion that the clay, below the fill and crust, is fairly homogeneous. A detailed study of each sample showed, however, a number of thin seams of sandy silt and even isolated pockets of quick clay, all in a very erratic pattern. The continuous sampling and closely spaced borings showed that there did not exist any continuity of the weaker seams of silt and sensitive clays to form continuous weak layers through the sliding mass. In fact, it is believed that these isolated irregularities do not invalidate the overall homogeneous character of the soil. However, these irregularities accounted for an occasional larger scatter in the index properties and in undrained strength on total stress basis (s_u-values).

By means of the unconfined compression tests and drop cone tests a large number of s_u-values was obtained (>1000). The scatter was very significant. For each 5 m depth interval mean values, standard deviations and hence variation coefficients were obtained. In Fig. 5 the black dots and vertical lines give the mean values for each interval, (at 73.7 m) and the dashed vertical lines indicate ± standard deviation. In general the coefficient of variation was found to be 0.4 - 0.5 for the compacted fill, and 0.25-0.35 for the intact clay. For each interval the number of measurements ranged between 14 and 26 for boring 74.7 m left. For comparison the mean values from borings 51.5 m left and 107.3 m left are also included in Fig. 5, based on 13 to 43 measurements for each depth interval. The coefficients of variation are similar for all borings.

Shear strength on total stress basis

For the Profile 3150 the undrained shear strength s_u, as obtained by drop cones, is illustrated in Fig. 6. For comparison a vane boring is also shown on this same profile. The s_u-values obtained from unconfined and vane tests are generally somewhat larger than the cone values.

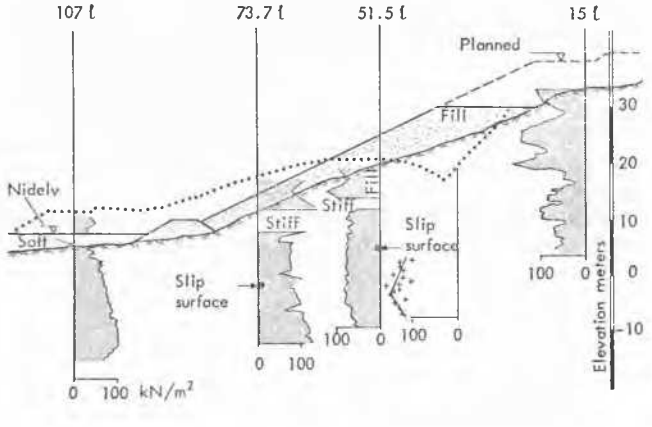

Fig.6 Simplified s_u - data along 3150

For calculatory purposes an overall average assessment would lead to $\bar{s}_u \cong 100$ kN/m² in the compacted fill, while for the intact clay

$$s_u = s_o + 0.3p_o' \qquad (1)$$

where p_o' = effective overburden before fill was placed, s_o = 60-70 kN/m² = value of s_u at original ground level. It is apparent that the above average s_u-values are uncertain measures of strength, as illustrated by the large coefficient of variation cited above.

Shear strength on effective stress basis

Altogether 35 triaxial tests were carried out, all as CU-tests, 21 isotropically consolidated (K_o) and 14 anisotropically consolidated at K_o', i.e. oedotriaxial tests. All tests were plotted as stress vectors (paths), i.e. $\frac{1}{2}(\sigma_1'-\sigma_3')$ versus σ_3'. For interpretations of the ICU-tests and Oedo-tests from such paths, see Refs. (3) and (5).

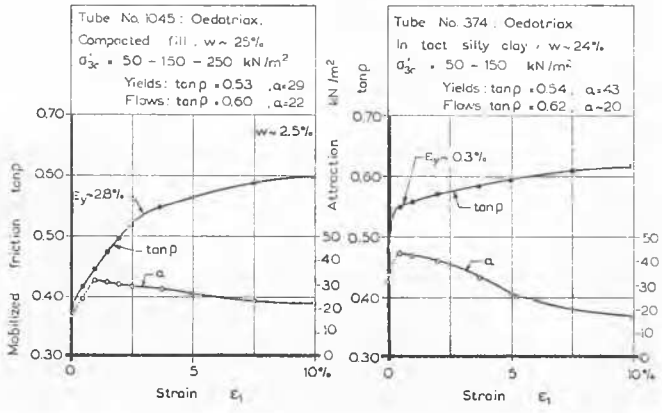

Fig.7 Mobilization curves for compacted fill and intact clay

Fig. 7 shows two typical mobilization curves for two series of oedotriaxial tests, one series for the compacted clay fill, and one for the intact clay. The mobilization curves show how attraction (a) and friction (tanρ) are being mobilized with increased strain ε_1, where

$$\tau_c = (a+\sigma_c') \tan\rho \qquad (2)$$

in which σ_c' = effective normal stress and τ_c = shear stress, both on the critical plane where F = minimum. As "failure" is approached $\tau_c \longrightarrow \tau_f$ when $\tan\rho \longrightarrow \tan\phi$. Both curves indicate a "yield" point for the same tanρ, the difference being that the intact soil reaches yield at a much smaller strain (1%) than the compacted fill (~3%) (young soil). Moreover, attraction is somewhat larger for the intact clay. The "ultimate failure", corresponding to approximately constant parameters (a and tanφ) are reached for large strains (~10%) and the parameters are then nearly equal for the fill and the intact clay. Note, however, that for the intact clay attraction is being broken down as strain increases (from 43 to 17 kN/m² for ε_1 = 1%-10%). The authors believe this is due to a gradual breakdown of the old geological bonds within the clay structure. This belief is supported by the entirely different behaviour of the fill, with fairly constant a over large ε_1-variations.

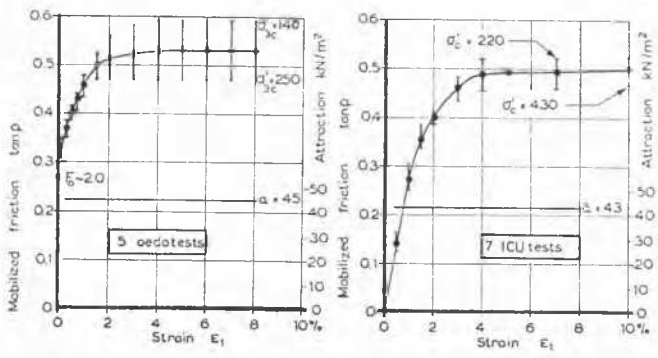

Fig.8 Average mobilization curves for 5 single oedotriax and 7 single ICU - tests

Fig. 8 shows average mobilization curves for 7 ICU-tests and 5 Oedo-tests on intact clay. In both cases a constant, mean value of attraction is used. The applied consolidation pressure σ_{3c}' is indicated on both diagrams. Generally tanϕ is lower the higher the σ_{3c}'.

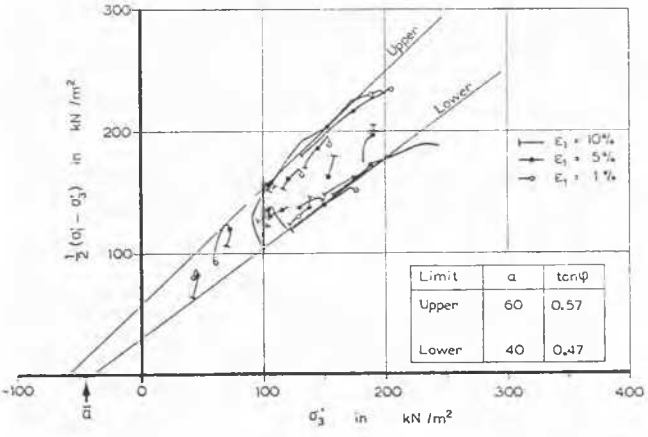

Fig.9 Stress paths for 17 triax on intact clay. Path for $\varepsilon_1 < 1\%$ left out to illustrate failure more clearly

The observed stress paths for all 17 triaxial tests on the intact clay are shown in Fig. 9. The "working stress range" of each path (i.e. $\varepsilon_1 < 1\%$) is left out to illustrate more clearly the soil behaviour at failure. This path assembly illustrates clearly that all 17 yield-flow paths from about $\varepsilon_1 = 1\%$ to 10% are located between a fairly narrow band defined by their limits

Upper: a = 60 kN/m³ tanϕ = 0.57

Lower: a = 40 kN/m³ tanϕ = 0.47

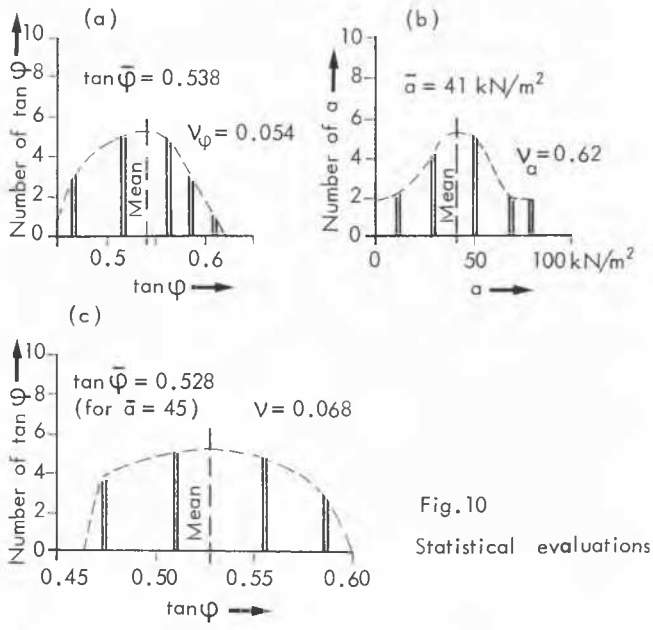

Fig.10 Statistical evaluations

A statistical analysis of single test a, ϕ-determinations lead to $\tan\bar{\varphi} = 0.538$ and $\bar{a} = 41$ with coefficients of variation $v_\varphi = 0.054$ and $v_a = 0.62$, respectively, see Fig. 10 ab. A lumped test determination with assumed $\bar{a} = 45$ yields $\tan\bar{\varphi} = 0.528$ with $v_\varphi = 0.068$, see Fig. 10c.

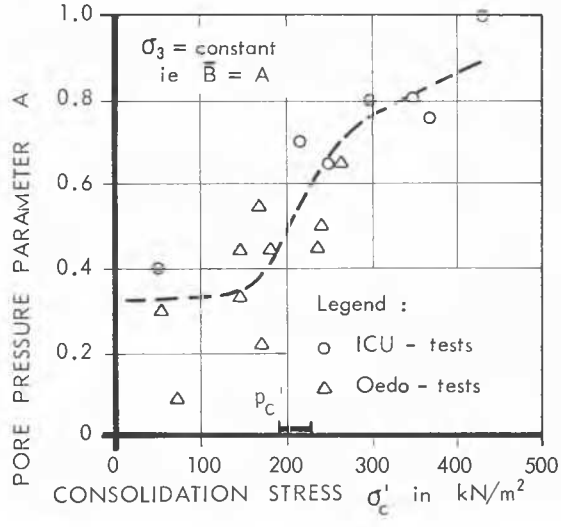

Fig.11 Measured A versus σ_c' for intact clay

The slopes of the stress paths in the working stress range define Skempton's pore pressure coefficient A. For tests with σ_3 = constant $A = \bar{B} = \Delta u/\Delta\sigma_1$. Fig. 11 shows that A is approximately equal to the elastic value (1/3) for $\sigma_c' < p_c'$ but increases rapidly towards 1.0 for $\sigma_c' >> p_c'$

STABILITY ANALYSIS

Very comprehensive stability analyses have been performed, out of which only a brief summary is given below.

Total stress analysis

The s_u-analysis, based on the average assessments of the s_u-profiles as given by Eq. (1), lead to F_{min} = 1.2 to 1.3 for s_o = 60 and 70 kN/m², respectively. The corresponding critical shear surfaces were, however, located far apart from the observed shear zones, or slip surface. More irregular, and layerwise, assumptions of average s_u lead essentially to the same result for F_{min}.

Effective stress analyses

The effective stress analyses (aϕ-analyses) involved the estimate of excess pore pressure due to the filling operation, assuming undrained conditions. The simplest estimate of Δu was based on the relationship

$$\Delta u = \bar{B}\Delta q \qquad (3)$$

where Δq = added weight by fill, $\bar{B}$ = Bishop's pore pressure coefficient.

The first aϕ-analyses were made with the aid of *stability charts* (see Ref. 1 and 2), as follows

$$F_{min} = N_{cf}\,\frac{a\tan\phi}{p_d} \qquad (4)$$

where p_d = total reference stress and N_{cf} = combined stability number depending on slope ratio b = tanβ and the dimensionless number

$$\lambda_{c\phi} = \frac{p_e}{a} \qquad (5)$$

where p_e = effective reference stress. The profile 3150 at Kroppan can be idealized to b = 2, H = 24 m and tail water H_w = 2 m, and

$$p_d = \gamma H - \gamma_w H_w$$
$$p_e = (1-\bar{r}_u)p_d \qquad (6)$$

where $\bar{r}_u$ = average u/γz-ratio.

Since γ = 20.5 kN/m², one gets p_d = 484 kN/m².

a	tanφ	$\frac{a\tan\varphi}{p_d}$	r_u	$\lambda_{c\varphi}$	N_{cf}	F_{min}
45 kN/m²	0.53	0.049	0.45	5.9	22.2	1.08
			0.50	5.4	21.1	1.03
			0.55	4.8	19.8	0.97
60 kN/m²	0.47	0.058	0.45	4.4	18.8	1.09
			0.50	4.0	17.6	1.02
			0.55	3.6	16.2	0.94

Table 1. Stability chart analysis, simplified profile

Table 1 shows the numerical analysis for $\bar{r}_u$ = 0.45, 0.50 and 0.55 for mean values of $\bar{a}$ = 45 and tan$\bar{\phi}$ = 0.53 and for a = 60 and tanϕ = 0.47. For $\bar{r}_u$ = 0.5 one gets F_{min} = 1.02 - 1.03 for both sets of parameters. A variation in $\bar{r}_u$ of ± 0.05 corresponds to an overall variation in pore pressure of ± 2 meters. Even this large variation in overall pore pressure means only ± 5 or 6% in estimated F_{min}. The critical shear surface (circle) for constant r_u is located somewhat above the observed slip surface. This is primarily due to the fact that the actual excess pore pressure due to the fill will be more consentrated towards the toe and less on the crest.

The Kroppan slide has also been analyzed by means of *Resistance Envelopes, or Critical Equilibrium Curves*. The last figure on page 81 in Ref. (1) is a dimensionless diagram with axes corresponding to:

$$\frac{\bar{\tau}}{p_d} = r_\tau \qquad \frac{\bar{\sigma}'}{p_e} = r_\sigma \qquad (7)$$

where $\bar{\tau}$ and $\bar{\sigma}'$ are the average shear stress and effective normal stress along a critical equilibrium curve ($\bar{\tau}$ vs $\bar{\sigma}'$) while p_d and p_e are the reference stresses defined above. Hence, for a given slope (b=2) with given p_d (484 kN/m²) one can construct $\bar{\tau}$-$\bar{\sigma}'$-curves for each chosen $\bar{r}_u$.

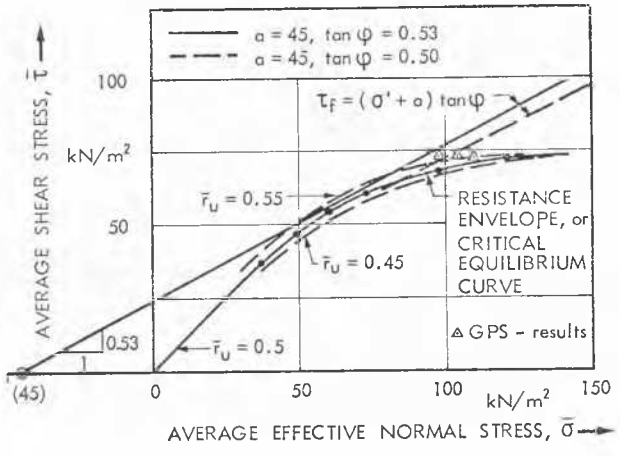

Fig.12 Critical equilibrium (resistance envelope) analysis of the Kroppan Slide

In Fig. 12 three such curves (for $\bar{r}_u$ = 0.55, 0.50 and 0.45) are shown, the middle one fully drawn, the two others are dashed. The shear strength lines for average $\bar{a}$ = 45 kN/m² and tanϕ = 0.53 and tanϕ = 0.50 are also drawn to compare with the critical equilibrium curves. It is seen that $\bar{\tau} \approx \tau_f$ (i.e. $F \equiv 1$) for a fairly large $\bar{\sigma}'$-variation when $\bar{r}_u$ = 0.45 - 0.55. This means that F≈1 for surfaces of different depths within say ± 2 meters. For comparison GPS are

included.

The Generalized Procedure of Slices was used extensively in analyzing the Kroppan slide.

More elaborate calculations of Δu could therefore be performed, based on the equation

$$\Delta u = \Delta\sigma_m - D\Delta\sigma_d \qquad (8)$$

where $\Delta\sigma_m$ = change in mean principal stress (octahedral), and $\Delta\sigma_d = \Delta(\sigma_1-\sigma_3)$ = change in deviator stress, D = dilatancy parameter. For elastic behaviour D = 0. The complete analysis required substantial trial and error.

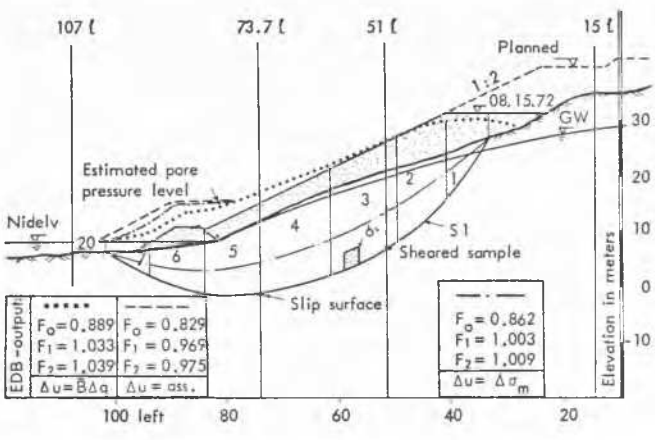

Fig.13 Stability analyses by the Generalized Procedure of slices (GPS)

Initially, Eq.(3)+(8) suggested a pore pressure level as indicated by the dotted curve in Fig. 13, and for this case the GPS-procedure (Ref. 4) leads to F = 1.04 for the observed slip surface, and using the average shear strength parameters found for the fill, the dry crust, and the intact clay respectively.

A more comprehensive parameter study, in which D, a and tanϕ have been varied between mean values ± standard deviation leads to a several meter wide zone within which F_{min} varied roughly between 0.95 and 1.05. This critical shear zone is very similar to the slip surface in shape and location. However, the bulk of the numerous shear surfaces where $F_{min} \sim 1.0$ are somewhat more shallow (2-3 m) than the actual depth of the slide. The authors believe this may be due to the fact that the actual excess pore pressure below the toe fill probably increased with depth, instead of being constant, as assumed in our analyses. Moreover, the higher the stress level, the larger a and the smaller tanϕ, i.e. the deeper the slide.

Therefore, a larger pore pressure level at the toe was assumed, see dashed level in Fig. 13. This lead to a factor of safety of about 0.98.

In order to investigate the pore pressure condition under the toe in greater detail the total normal stress changes along the slip surface were obtained by the GPS-procedure. Assuming the OC-clay to behave elastically (i.e. D=0) and taking $\Delta\sigma_m$ equal to Δσ along the slip surface, a new pore pressure level under the toe was found, (see dash-dotted level in Fig. 13). With this new pore pressure level a factor of safety of 1.01 was found. The corresponding normal and shear stress along the slip surface, and the interslice forces are shown in Fig. 14, together with the estimated $\Delta\sigma \equiv \Delta\sigma_m$ along the same surface, as compared to $\Delta q = \gamma_{fill} \cdot H_{fill}$.

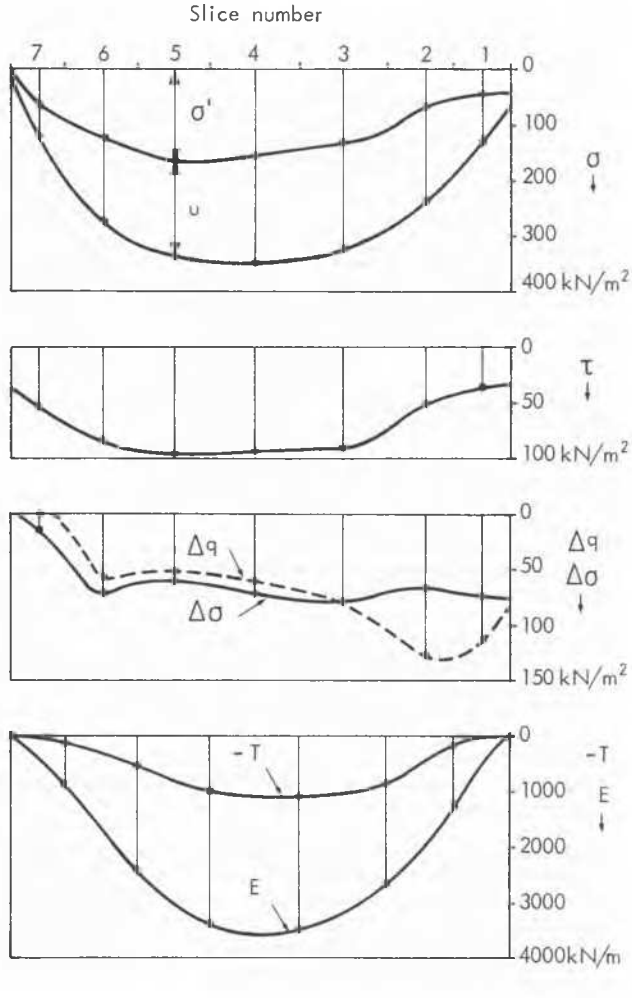

Fig.14 Stresses along shear surface, and interslice forces.

CONCLUDING REMARKS

The most important message learned from the very extensive investigation of the Kroppan slide is the following:

> The short-term, undrained stability of an overconsolidated clay beneath a road embankment was accurately revealed by means of effective stress analysis ($a\phi$-analysis). By contrast, a total stress analysis (s_u-analysis) gave misleading information about the location of the critical shear zones as well as the safety.

The short-term $a\phi$-analyses required the prediction of the excess pore pressure due to the embankment load. The uncertainty still associated with such pore pressure predictions does not invalidate the above statement, simply because the influence of the remaining uncertainties on the safety factor is remarkably small, say within $\pm$ 5 to 6% for the Kroppan slide.

ACKNOWLEDGEMENT

The authors would like to acknowledge the extensive help they received from a number of their colleagues in the two organizations behind this large investigation, and from the two students at the time, R.H. Johnsen (triaxial tests) and I. Horvli (numerical analysis). Especially, our gratefulnes goes to chief engineer N. Rygg, Norwegian Road Research Laboratory, who was in charge of and organized the investigations.

APPLIED REFERENCES

Pore pressure parameters A and $\bar{B}$ and pore pressure coefficient r_u defined in:

Bishop, A.W.:

"The use of pore pressure coefficients in practice". Geotechnique, Volume 4,1954.

Bishop, A.W. and Morgenstern, N.:

"Stability coefficients for earth slopes". Geotechnique, Volume X, 1960.

Skempton, A.W.:

"The pore pressure coefficients A and B". Geotechnique, Volume 4, 1954.

The paper is otherwise based on three extensive reports prepared under the guidance of the authors, and on two diploma theses at NTH, i.e. by Johnsen and Horvli. The triaxial test interpretations and the stability analysis were based on the following papers by the senior author:

(1) "Stability analysis of slopes with dimensionless parameters", Harvard University SM Series No. 46, 1954, 81 pages.

(2) "Dimensionless parameters for homogeneous earth slopes". Discussion ASCE, SM, No. 1967, pp 367-374.

(3) "Shear strength and stability of soils", NGF-foredraget, NGI, Oslo, 48 pages.

(4) "Slope stability computations" from "Embankment-Dam-Engineering" - the Casagrande Volume, Wiley International, 1973, pp 47-86.

(5) "Skjærstyrken av granulære materialer", Nordisk geoteknikermøte, NGM 75, Polyteknisk Forlag, Copenhagen, pp 37-50.